International Journal of Theoretical Physics, Vol. 35, No. 1, 1996

Classical Irreversibility and Mapping of the Isosceles Triangle Billiard

Richard L. Liboff[1]

Received April 3, 1995

Mapping of the two-dimensional isosceles triangle billiard onto the circular one-dimensional motion of two mass points is described. The singular nature of trajectories directly incident on an acute vertex is discussed in the framework of the present mapping. For an obtuse-angled isosceles triangle, dynamical equations in two-particle space applied to an orbit along a hypotenuse incident on the obtuse vertex suggests irreversible behavior at the critical angle $\psi = 2\pi/3$. Thus it is found that the nonsingular motion of a finite smooth-walled disk on this trajectory exhibits irreversibility. A finite spherical smooth-walled particle moving in a uniform right cylinder whose cross section includes this critical vertex angle likewise exhibits irreversibility. Each such example comprises an irreversible orbit for a single-particle Hamiltonian.

1. INTRODUCTION

A mapping of the isosceles triangular billiard onto the motion of two impenetrable mass points moving on a circle with particle displacement equal to respective arc lengths is described. The related one-dimensional motion corresponds to respective angular displacements of the two particles. This mapping is one-to-one save for the set of points comprising the bisecting line of the triangle. However, any two-particle state in one-dimensional circular space maps onto only one state in the corresponding triangular billiard domain. The mapping is a generalization of Sinai's map (Sinai, 1976; Cornfeld *et al.*, 1982; Katok and Strelcyn, 1986) of the right-triangular billiard. In accord with the Sinai map, the two equal legs of the isosceles triangle are each labeled a hypotenuse. It is noted that a trajectory along a hypotenuse in collision with the obtuse vertex at the critical angle $\psi = 2\pi/3$ constitutes

[1] Schools of Electrical Engineering and Applied Physics and Center for Applied Mathematics, Cornell University, Ithaca, New York 14853.

0020-7748/96/0100-0189$09.50/0

an irreversible, but singular orbit (Liboff, 1987, 1990a,b; Reichl, 1990). It is shown that the nonsingular corresponding motion of a finite smooth-walled disk is irreversible and that the singular point-particle irreversible trajectory follows in the limit as the radius of the disk reduces to a point. Each such sequential trajectory is a solution to dynamical equations for a Hamiltonian and is an irreversible orbit. This irreversibility is found likewise to apply to a smooth-walled finite spherical particle moving in a uniform right cylinder whose cross section includes the critical vertex angle. For both these latter examples, reflection at the vertex occurs from a wall, not from the vertex as is the case for a point particle. Apart from abstract mathematical modeling (Hasegawa and Driebe, 1992, 1993), no previous study has demonstrated irreversibility of a physical system with few degrees of freedom.

The singular nature of trajectories directly incident on an acute vertex is discussed in the framework of the present mapping. Three sets of such direct vertex scatterings are introduced, of varying degrees of singularity. Working in the representation of the present mapping, it is found that such orbits retroreflect.

2. BILLIARD CONFIGURATION

The billiard configuration we wish to consider is that of an isosceles triangle oriented as shown in Fig. 1, in Cartesian y space, with the base of the triangle aligned with the $y_1 = 0$ line. At any instant of time the billiard particle has Cartesian components (y_1, y_2). The billiard's motion is mapped

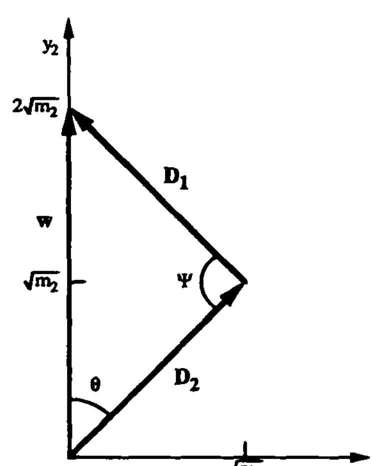

Fig. 1. Isosceles triangular billiard configuration with defined hypotenuse vectors $\mathbf{D}_1$ and $\mathbf{D}_2$ and the nonhypotenuse leg $\mathbf{w}$.

onto the one-dimensional motion of two particles of dimensionless masses (m_1, m_2) and respective displacements (x_1, x_2) through

$$y_1 = \sqrt{m_1}x_1$$
$$y_2 = \sqrt{m_2}x_2 \tag{1a}$$

where

$$0 \leq x_1 \leq 1, \qquad 0 \leq x_2 \leq 2 \tag{1b}$$

As illustrated in Fig. 1, the triangle includes two "hypotenuses" defined by

$$\mathbf{D}_2 = (\sqrt{m_1}, \sqrt{m_2}) \tag{2a}$$
$$\mathbf{D}_1 = (-\sqrt{m_1}, \sqrt{m_2}) \tag{2b}$$

The angle between the $y_1 = 0$ leg and either hypotenuse is $\theta = \tan^{-1} (m_1/m_2)^{1/2}$. Conservation of energy of the particle in collision with either hypotenuse is given by the relations

$$E = m_1\dot{x}_1^2 + m_2\dot{x}_2^2 = \dot{y}_1^2 + \dot{y}_2^2 = \dot{y}^2 = \dot{y}'^2 \tag{3a}$$

Conservation of momentum in the direction of a hypotenuse is given by

$$\dot{\mathbf{y}} \cdot \mathbf{D} = \dot{\mathbf{y}}' \cdot \mathbf{D} \tag{3b}$$

where $\mathbf{D}$ is written for $\mathbf{D}_1$ or $\mathbf{D}_2$. In the preceding relation, E is a constant of the mapping, primed values denote after collision, and a dot denotes time differentiation.

To incorporate the condition (1b) into the present mapping, the m_1 and m_2 particles are constrained to move on a circle with respective arc-length displacements (x_1, x_2). One point on the circle, labeled W (Fig. 2), corresponds

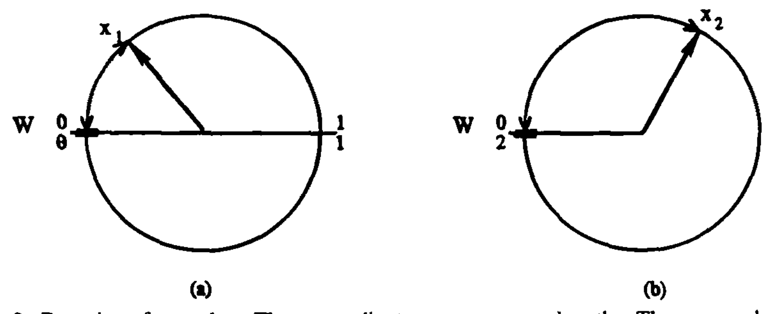

(a) (b)

Fig. 2. Domains of x_1 and x_2. These coordinates represent arc lengths. The arrows drawn to x_1, x_2 from the origin are for clarity. The reflecting wall W at $x_1 = x_2 = 0$ is shown.

to the impenetrable nonhypotenuse leg at $y_1 = 0$, labeled **w** (Fig. 1). In the upper-half circular B_x domain

$$0 \leq x_1 \leq x_2 \leq 1 \tag{4a}$$

while in the lower-half circular A_x domain

$$0 \leq x_1 \leq 1, \qquad 1 \leq x_2 \leq 2 \tag{4b}$$

(Fig. 3). Thus, in each domain of the circle, $x_1 \leq x_2$ (corresponding to $m_1 \leq m_2$, and $\theta \leq \pi/4$ in y space). In both halves of the circle, reflection of $\dot{x}_1$ from the point W in x space corresponds to reflection from **w** in y space. In each such collision in x space (with $x_1 < x_2$) $\dot{x}_1$ reverses and $\dot{x}_2$ maintains (at the instant of the $\dot{x}_1$ reversal). Reflection from a hypotenuse in y space corresponds to collision of particles in x space at a point on the circular domain away from the W point.

This mapping is one-to-one, except for states on the line $y_2 = \sqrt{m_2}$, for which y states may be said to be twofold degenerate. That is, any point on this line maps onto two points in x space which are mirror images about the diameter through the point $x_2 = 1$. Thus, in the mapping to x space of the periodic motion along $y_2 = \sqrt{m_2}$, symmetric trajectories of these mirror-image particles begin at W, simultaneously collide with the stationary m_2 particle at $x_2 = 1$, and symmetrically reflect back to W.

Whereas our generalized Sinai mapping from y to x space is not one-to-one, the reverse mapping is one-to-one. That is, any point in x space maps onto only one point in y space, so that the dynamics of the two-particle motion in x space uniquely maps onto the corresponding billiard motion in y space.

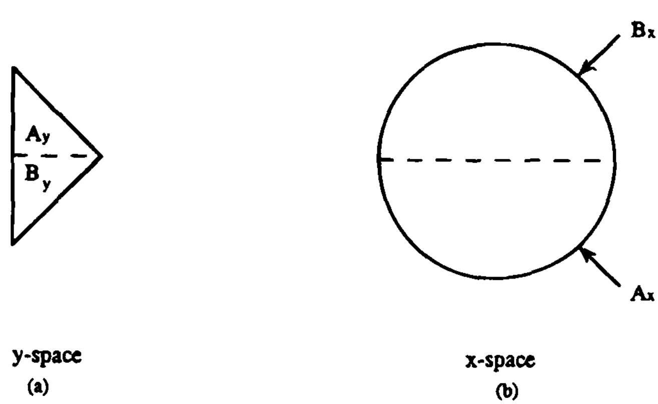

Fig. 3. (a) Triangle y space. (b) Circle x space.

3. DYNAMICAL EQUATIONS AND TRAJECTORIES

3.1. Crossover Rules

Let A_y and B_y, respectively, represent the upper and lower right-triangular halves of the isosceles domain in y space (Fig. 3). As described above, states and trajectories in the domains A_x and B_x map uniquely onto corresponding states and trajectories in the A_y and B_y domains. Trajectories in these two domains of the two point-masses (m_1, m_2) with respective coordinates (x_1, x_2) are determined by the one-dimensional dynamical equations

$$\dot{x}_1' = \frac{m_1 - m_2}{M}\dot{x}_1 + \frac{2m_2}{M}\dot{x}_2$$

$$\dot{x}_2' = \frac{m_2 - m_1}{M}\dot{x}_2 + \frac{2m_1}{M}\dot{x}_1 \tag{5}$$

where $M = m_1 + m_2$ and primed variables represent values after collision. Dynamics through the point $x_2 = 1$ (corresponding to motion through the bisecting line of the triangle in y space) is given by the following rules: Consider trajectories which cross from the B_x domain to the A_x domain through this point. At the value $x_2 = 1^-$, x_1 reflects through the diameter (which includes the point $x_2 = 1$) to the A_x domain, with continuous motion maintained. For example, if $\dot{x}_1 > 0$, then this value is maintained through the crossover. Similarly, for a trajectory in A_x, at the value $x_2 = 1^+$, x_1 reflects to the image point in the B_x domain with continuous motion maintained. The event which follows a crossover of x_1, for $\dot{x}_1 > 0$, corresponds in y space to reflection from the respective $\mathbf{D}_1$ or $\mathbf{D}_2$ hypotenuse subsequent to which there is a collision with $\mathbf{w}$. Note that continuous motion, both in x and y space, is maintained through the crossover event.

In applying the dynamical equations (5) in the domain A_x or the momentum conservation equation (2b), (3b) in this domain, the following important rule should be noted: as the sign of increase of x_1 is opposite to that of x_2 in A_x, for consistency of application of these dynamical equations in this domain, the signs in front of $\dot{x}_1$ and $\dot{x}_1'$ are reversed. Thus, for example, with the transformation equations (1a), (2b), (3b), relevant to domain A_x, one obtains conservation of momentum with the noted sign changes. Motion along either hypotenuse in y space corresponds to coincident motion of x_1 and x_2 in x space. For motion on $\mathbf{D}_1$, sign-change rules apply and one obtains $\dot{x}_1 = -\dot{x}_2$, which with (1a) returns the correct corresponding relation in y space.

Here is an additional simple application of rules of the preceding mapping which demonstrates their consistency. Consider the equilateral triangle billiard for which $m_1 = 3/4$, $m_2 = 1/4$. Let us examine the initial velocities $\dot{x}_1 = 0$

and $\dot{x}_2 = -a$, which correspond in y space to the particle vertically incident on $\mathbf{D}_2$. Equations (5) give the reflected velocities

$$\dot{x}_1' = -\frac{a}{2} \rightarrow \dot{y}_1' = -\frac{a}{4}\sqrt{3}$$
$$\dot{x}_2' = \frac{a}{2} \rightarrow \dot{y}_2' = \frac{a}{4} \tag{6}$$

The slope of the reflected orbit in y space is $-1/\sqrt{3}$ corresponding to linear motion parallel to $\mathbf{D}_1$. Repeating this calculation for vertical incidence on $\mathbf{D}_1$ gives reflection parallel to $\mathbf{D}_2$. Reversing the first orbit and combining with the second orbit gives a net "juxtareflected" trajectory (i.e., switching of incident motion parallel to $\mathbf{D}_1$ to reflected motion parallel to $\mathbf{D}_2$). Such motion maintains as the first point of reflection approaches the vertex and we may conclude that juxtareflection is consistent for a particle incident on a leg of a vertex of angle $\pi/3$. In each such event the particle experiences two bounces.

Retroreflection or juxtareflection from an acute-angled vertex for incident motion parallel to a leg of the vertex occurs for vertex angles π/n, where $n \geq 2$ is an integer. This may be seen through mapping the orbit onto a straight line in the plane (comprised of $2n$ congruent wedges with a common vertex at the origin) (Koslov, 1991; Kerckhoff *et al.*, 1986).

3.2. Acute Vertex Scattering

Vertex reflections discussed above are multibounce events. In the limit that the first bounce of such an event approaches the vertex, the bounce number of the reflection maintains. Direct incidence of a trajectory on a vertex is a single-bounce scattering and is singular event (Koslov, 1991). This singular property is well illustrated in x space. Thus, any collision on the acute vertex, say, at (0, 0) in y space, corresponds to x_1 and x_2 simultaneously incident on W. Any deviation of simultaneous collision of x_1 and x_2 with W, no matter how small, corresponds to multi-wall reflections in y space.

Within the framework of the present mapping, it is possible to discuss properties of such singular direct-vertex scatterings. Thus, for scattering from either acute vertex ($\theta \leq \pi/4$), we note the following: As noted above, any trajectory incident on, say, the acute vertex at (0, 0) in y space corresponds in x space to x_1 and x_2 simultaneously incident on W from which both particles reflect with individually reversed speeds. It follows that a point particle directly incident on either acute vertex retroreflects. Two examples of this rule are as follows. Consider the trajectory in y space $y_1 = 0$, $y_2 > 0$, $\dot{y}_2 < 0$ corresponding to motion along the $y_1 = 0$ leg toward (0, 0). In the corresponding situation in x space, $\dot{x}_2$ reverses in collision with W and x_1 remains at W. In the related situation in y space, the particle retroreflects. Next consider the trajectory in y space along $\mathbf{D}_2$ toward (0, 0). In x space the two particles are coincident. At W the coincident particles simultaneously reflect and again the particle in y space retroreflects. For the subset of angles $\theta = \pi/n$, where again $n \geq 2$ is an integer, this result may be established as described above through mapping the orbit onto a straight line in the plane. Retroreflection for direct vertex scattering follows in the limit that the trajectory line passes through the origin. Any variation of the straight line from the origin, no matter how small, results in a multibounce scattering, again revealing the singular nature of these events.

Retroreflection of direct vertex scattering, when viewed in x–t space, with $x_1(t)$ and $x_2(t)$ superimposed, illustrates the dynamic reversibility of these orbits (Fig. 4).

3.3. I and L Scattering Events

We introduce the following sets of vertex scattering events. In **I** scatterings, the incident trajectory lies in the open domain of the triangle. As noted above, except for a subset of measure zero, all scatterings in the **I** set are singular. In $\mathbf{I}_b$ scatterings, the incident trajectory bisects the vertex. From symmetry, the particle retroreflects. Replacing the point particle by a disk of finite radius likewise gives retroreflection. In the limit that the radius of the disk shrinks to a point this property maintains. Thus, we classify $\mathbf{I}_b$ scattering as quasisingular, as it is still the case that any variation of the trajectory away from the vertex, no matter how small, destroys the retroreflection. In **L** scattering, the incident trajectory is along a leg of the vertex. As the incident particle is so constrained, such scattering events are nonsingular. For direct vertex incidence on an acute vertex, **L** scattering results in retroreflection.

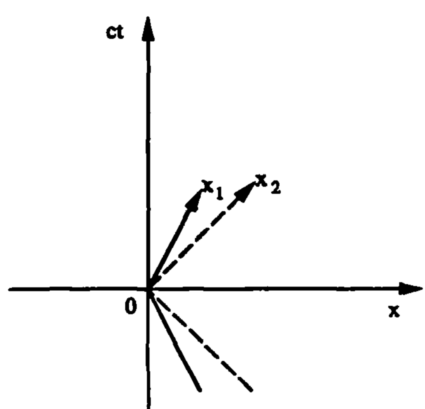

Fig. 4. Direct vertex scattering in x–t space from the W point (labeled 0) illustrating dynamic reversibility of the retroreflected orbit in y space. The parameter c is a characteristic speed.

This is shown as follows. Consider a smooth-walled disk of finite radius on $\mathbf{D}_2$ which moves toward the vertex with $\mathbf{w}$. At the vertex the impact force on the disk is normal to $\mathbf{w}$ and passes through the center of the disk. Due to the constraint of the $\mathbf{D}_2$ wall, the disk retroreflects in response to the component of force parallel to $\mathbf{D}_2$. This construction maintains as the radius of the disk shrinks to a point.

3.4. Obtuse-Vertex Scattering

We concentrate on $\mathbf{L}$ scattering in which the particle in y space is directed toward the obtuse vertex ($m_1 \leq m_2$) along a hypotenuse leg of the triangle. For this case, a trajectory on $\mathbf{D}_2$ toward the obtuse vertex specularly reflects at the vertex from $\mathbf{D}_1$. This conclusion follows as in the limiting cases considered above. Thus, again consider that a finite, smooth-walled disk on $\mathbf{D}_2$ moves toward the obtuse vertex with $\mathbf{D}_1$. In this case, the $\mathbf{D}_2$ wall merely guides the disk to its collision with $\mathbf{D}_1$ at which point the impact force on the disk is due entirely to $\mathbf{D}_1$. This conclusion remains valid as the radius of the disk shrinks to a point.

Depending on whether $\psi < 2\pi/3$ or $\psi > 2\pi/3$, the particle then enters the $\mathbf{B}_y$ or $\mathbf{A}_y$ domain, respectively. To examine this situation in x space we set $x_2 = x_1 + \epsilon$ and let $\epsilon \to 0$. The critical angle $\psi = 2\pi/3$ follows from applying (5) with the sign-change rules stated above. We obtain

$$\dot{x}_1' = \left(\frac{m_1 - 3m_2}{M}\right)\dot{x}_1$$

$$\dot{x}_2' = \left(\frac{m_2 - 3m_1}{M}\right)\dot{x}_2 \qquad (7)$$

A particular solution of these relations is employed below in the description of an irreversible orbit.

4. IRREVERSIBLE ORBITS

4.1. Point Particle

For the configuration considered immediately above, the initial trajectory on $\mathbf{D}_2$ toward the obtuse vertex corresponds to values $\dot{x}_1 = \dot{x}_2 > 0$. The critical mass ratio implied by (7) is $m_1/m_2 = 1/3$. With this property and the given initial conditions, (7) yields the values $\dot{x}_2' = 0, \dot{x}_1' < 0$, which correspond in y space to reflection from $\mathbf{D}_1$ onto the symmetry line separating $\mathbf{A}_y$ and $\mathbf{B}_y$. The resulting periodic orbit is an $\mathbf{I}_b$ trajectory, as it bisects the obtuse vertex and reflects normally from $\mathbf{w}$. As noted above, $\mathbf{I}_b$ trajectories may be considered to be quasisingular. Reversing this orbit at any instant never recaptures the reverse of the starting trajectory on the hypotenuse, and we may conclude that this quasisingular trajectory is irreversible (Liboff, 1987, 1990a,b; Reichl, 1990).

4.2. Finite Disk and Finite Sphere

The nonsingular motion of a smooth-walled disk of finite radius, starting with the same initial conditions as described immediately above, experiences the same irreversibility. In this case reflection is from the $\mathbf{D}_1$ wall at a finite displacement from the vertex. The singular irreversible trajectory of a point particle occurs in the limit that the radius of the disk shrinks to a point.[2]

This irreversibility applies equally to a finite, smooth-walled spherical particle moving within a uniform right, smooth-walled cylinder whose cross section includes a vertex of critical angle, $2\pi/3$. The radius of the particle is small compared to the mean diameter of the cylinder. Consider a trajectory along a side of the cylinder in the vicinity of the critical vertex which moves toward the vertex. The component of this motion in a cross-sectional plane of the cylinder reveals the irreversibility of the orbit. For either the two-dimensional finite-disk motion or the three-dimensional finite-sphere motion, the Hamiltonian of the system occurs with time-invariant boundary conditions.

5. CONCLUSIONS

A mapping is described in which the isosceles triangle billiard is mapped onto the motion of two mass points moving on a circular one-dimensional curve, with particle displacements given by respective arc lengths along the circle. The singular nature of trajectories directly incident on an acute vertex is discussed in the framework of the present mapping. Working in this representation, it is found that these orbits retroreflect. A trajectory classification scheme is introduced related to such direct vertex scatterings. For an obtuse-angled isosceles triangle, dynamical equations in two-particle x-space applied to an orbit in triangle space along a hypotenuse incident on the obtuse vertex imply a separation of reflected orbits at the critical obtuse angle $\psi = 2\pi/3$. At this critical angle it is noted that the related singular orbit is irreversible. It is shown that the nonsingular motion of a finite smooth-walled disk likewise exhibits this irreversibility. The point-particle singular irreversible trajectory follows in the limit as the radius of the disk reduces to a point. Each such sequential trajectory is a solution to dynamical equations and is an irreversible

[2] In L scattering the vertex angle $\psi = 2\pi/3$ is the only angle for which the reversed orbit is affected by both legs of the vertex. For all other vertex angles in the interval $\pi/2 \leq \psi < \pi$, the reversed orbit is affected only by the original reflecting leg.

orbit. This irreversibility applies also to the nonsingular motion of a finite spherical particle moving in a uniform right cylinder whose cross section includes a critical vertex angle.

ACKNOWLEDGMENTS

I am indebted to John Smillie for introducing me to the Sinai map and to Matthew Angyal, Kaushik Bhaumik, Greg Ezra, David Emerson, Wolfgang Hofmann, George George, Hercules Neves, Volkan Kaman, Jeffrey Ng, and Kerry Litvin for fruitful discussions on this topic. I am particularly indebted to Paul Swanson for discussions related to the irreversibility of the critical orbit and to Gregory Dionne and Joseph Digioia for their very careful reading of the manuscript and constructive criticism.

REFERENCES

Cornfeld, I. P., Fomin, S. V., and Sinai, Ya. G. (1982). *Ergodic Theory,* Springer-Verlag, New York.

Hasegawa, H. H., and Driebe, D. J. (1992). *Physics Letters A,* **168**, 18.

Hasegawa, H. H., and Driebe, D. J. (1993). *Physics Letters A,* **176**, 193.

Katok, A. B., and Strelcyn, J.-M. (1986). *Invariant Manifolds, Entropy and Billiards,* Springer-Verlag, New York.

Kerckhoff, S., Masur, H., and Smillie, J. (1986). *J. Ann. Math.* **124**, 293.

Kozlov, V. (1991). *Billiards: A Generic Introduction to the Dynamics of Systems with Impacts,* AMS, Providence, Rhode Island.

Liboff, R. L. (1987). *Journal of Physics A,* **20**, 5607.

Liboff, R. L. (1990a). *Kinetic Theory: Classical, Quantum and Relativistic Descriptions,* Prentice-Hall, Englewood Cliffs, New Jersey, Section 3.3.5.

Liboff, R. L. (1990b). *Journal of Non-Equilibrium Thermodynamics,* **15**, 15.

Reichl, L. E. (1980). *A Modern Course in Statistical Physics,* University of Texas Press, Austin, Texas, Chapter 8.

Sinai, Ya. G. (1976). *Introduction to Ergodic Theory,* Princeton University Press, Princeton, New Jersey.